Title

Alcaligenes lipid A functions as a superior mucosal adjuvant to monophosphoryl lipid A via the recruitment and activation of CD11b+ dendritic cells in nasal tissue.

Journal

International Immunology, 36(1)

Authors

Sun, Xiao

Hosomi, Koji

Shimoyama, Atsushi

et al.

Publication Date

2024-01-29

DOI

10.1093/intimm/dxad045

Peer reviewed

International Immunology, Vol. 36, No. 1, pp. 33–43
https://doi.org/10.1093/intimm/dxad045
Advance Access publication 25 November 2023

REVIEW

Alcaligenes lipid A functions as a superior mucosal adjuvant to monophosphoryl lipid A via the recruitment and activation of CD11b$^+$ dendritic cells in nasal tissue

Xiao Sun[1,2], Koji Hosomi[1], Atsushi Shimoyama[3,4], Ken Yoshii[1,5], Azusa Saika[1], Haruki Yamaura[3], Takahiro Nagatake[1,6], Hiroshi Kiyono[7,8,9,10], Koichi Fukase[3,4] and **Jun Kunisawa[1,2,3,4,5,11,12,13,14]**

[1]Laboratory of Vaccine Materials and Laboratory of Gut Environmental System, Microbial Research Center for Health and Medicine, National Institutes of Biomedical Innovation, Health and Nutrition (NIBIOHN), Osaka 567-0085, Japan
[2]Graduate School of Pharmaceutical Sciences, Osaka University, Suita, Osaka 565-0871, Japan
[3]Department of Chemistry, Graduate School of Science, Osaka University, Osaka 560-0043, Japan
[4]Collaborative Research Between NIBIOHN and Graduate School of Science, Forefront Research Center, Osaka University, Osaka 560-0043, Japan
[5]Graduate School of Medicine, Osaka University, Osaka 565-0871, Japan
[6]Department of Life Sciences, Laboratory of Functional Anatomy, School of Agriculture, Meiji University, Kanagawa 214-8571, Japan
[7]Division of Gastroenterology, Department of Medicine, University of California San Diego (UCSD), San Diego, CA 92093, USA
[8]Chiba University (CU)-UCSD Center for Mucosal Immunology, Allergy and Vaccines (cMAV), UCSD, San Diego, CA 92093-0063, USA.
[9]Future Medicine Education and Research Organization, Chiba University, Chiba 260-8670, Japan
[10]Department of Human Mucosal Vaccinology, Chiba University Hospital, Chiba 260-8677, Japan
[11]International Vaccine Design Center, The Institute of Medical Science, The University of Tokyo, Tokyo 108-8639, Japan
[12]Department of Microbiology and Immunology, Kobe University Graduate School of Medicine, Kobe 650-0017, Japan
[13]Research Organization for Nano and Life Innovation, Waseda University, Tokyo 162-0041, Japan
[14]Graduate School of Dentistry, Osaka University, Suita 565-0871, Japan.

Correspondence to: J. Kunisawa; E-mail: kunisawa@nibiohn.go.jp

Received 18 June 2023, *editorial decision* 16 November 2023, *accepted* 24 November 2023

Abstract

We previously demonstrated that *Alcaligenes*-derived lipid A (ALA), which is produced from an intestinal lymphoid tissue-resident commensal bacterium, is an effective adjuvant for inducing antigen-specific immune responses. To understand the immunologic characteristics of ALA as a vaccine adjuvant, we here compared the adjuvant activity of ALA with that of a licensed adjuvant (monophosphoryl lipid A, MPLA) in mice. Although the adjuvant activity of ALA was only slightly greater than that of MPLA for subcutaneous immunization, ALA induced significantly greater IgA antibody production than did MPLA during nasal immunization. Regarding the underlying mechanism, ALA increased and activated CD11b$^+$ CD103$^-$ CD11c$^+$ dendritic cells in the nasal tissue by stimulating chemokine responses. These findings revealed the superiority of ALA as a mucosal adjuvant due to the unique immunologic functions of ALA in nasal tissue.

Keywords: Alcaligenes, chemokines, lipid A, MPLA, nasal vaccine, stromal cells

Introduction

Currently, most vaccines are administered subcutaneously or intramuscularly to induce potent systemic immunity (1), but these vaccines produce only weak mucosal immunity (2). In contrast, oral and nasal mucosal vaccines can induce both mucosal and systemic immunity (3). Because the mucosal tissues are the first line of defense against many pathogens, the mucosal immunity induced by mucosal vaccines is superior to that from systemic vaccines in terms of the protection against various pathogens that invade through mucosal tissues (3), such as influenza (4), coronavirus disease (COVID-19) (5), and human immunodeficiency virus (6). These properties of mucosal vaccines make them more advantageous than other types of vaccines. Currently, eight licensed oral vaccines are available (which prevent cholera, salmonella, poliovirus, and rotavirus), but only a single intranasal vaccine (against influenza) is approved for clinical use (7). Several additional mucosal vaccines are in development or clinical trials (8, 9).

Among the components of vaccination, the adjuvant is an indispensable element, which can enhance innate and adaptive immunity (10). To achieve successful immunity in the host, injection-type vaccines require the use of an effective and safe adjuvant. Current candidate adjuvants include those carrying danger-associated molecular patterns and pathogen-associated molecular patterns (11). Among them, monophosphoryl lipid A (MPLA) from *Salmonella minnesota* R595 is a licensed adjuvant used in the human papillomavirus (12) and hepatitis B virus (13) vaccines. MPLA exerts its adjuvant activity by recognizing Toll-like receptor 4 (TLR4) on antigen-presenting cells, such as dendritic cells (DCs), and enhancing innate immunity (14, 15). Activated DCs subsequently prime $CD4^+$ and $CD8^+$ T-cell responses to boost adaptive immunity (14, 16). This process improves immune responses against antigens and establishes immunologic memory.

In our previous reports, we identified a commensal bacterium, *Alcaligenes* spp., in the gut-associated lymphoid tissue of Peyer's patches (17). A membrane component of *Alcaligenes*, lipopolysaccharide (LPS), and its active site, lipid A (ALA), showed sufficient safety in subcutaneous and intranasal vaccination and exerted potent adjuvanticity through the recognition of TLR4 (18–21). *Alcaligenes* LPS was confirmed to be a mild agonist of TLR4, thus inducing only low-grade DC-mediated inflammatory responses, such as proinflammatory cytokine production and nitric oxide generation (22). Synthetic ALA had a similar effect to *Alcaligenes* LPS (23), activating DCs as an adjuvant with minimal inflammatory response (19). In particular, ALA protected against respiratory infection due to *Streptococcus pneumoniae* in a mouse model (20). These results imply that ALA could be an effective systemic and mucosal vaccine adjuvant.

The MPLA in clinical use has not been tested for adjuvant efficacy with mucosal vaccines. In this study, we compared the adjuvant activity of ALA and MPLA for intranasal administration in mice and investigated the mechanisms underlying these effects.

Methods

Mice

BALB/cAJcl mice were purchased from CLEA Japan, Inc. (Tokyo, Japan) and housed under specific pathogen-free conditions at the National Institutes of Biomedical Innovation, Health, and Nutrition (Osaka, Japan). All experiments were approved by the Animal Care and Use Committee of the National Institutes of Biomedical Innovation, Health, and Nutrition and were conducted according to their guidelines.

Lipid A

Alcaligenes lipid A (ALA) was chemically synthesized as described previously (23). MPLA from *Salmonella minnesota* R595 was purchased from InvivoGen (San Diego, CA, USA). Both adjuvants were reconstituted in dimethyl sulfoxide (Nacalai Tesque, Kyoto, Japan) at a concentration of 1 mg/ml and stored at −30°C.

Vaccination

For intranasal vaccination, mice were immunized with 5 μg of ovalbumin (OVA) with or without 1 μg of ALA or MPLA in 15 μl of phosphate buffered saline (PBS) on days 0, 7, and 14. At 7 days after the last immunization, we collected serum, nasal wash fluid, and bronchoalveolar lavage fluid from mice for measurement of OVA-specific immunoglobulin A (IgA) and IgG via enzyme-linked immunosorbent assay (ELISA). For subcutaneous vaccination, mice were immunized with 1 μg of OVA with or without 1 μg of ALA or MPLA in 200 μl of PBS on days 0 and 7. At 7 days after the last immunization, serum was collected from mice for OVA-specific IgG ELISA measurement.

Immunohistochemistry

Nasal-associated lymphoid tissue (NALT) and cervical lymph nodes (CLNs) from intranasally immunized mice were analyzed as described previously (20). Tissue samples were embedded in the Tissue-Tek O.C.T. Compound (Sakura Finetek Japan, Tokyo, Japan), frozen with liquid nitrogen, and stored at −80°C until use. Frozen samples were cut into 6-μm sections at −20°C by using a CM3050 S cryostat (Leica Biosystems, Wetzlar, Germany). Sections were fixed with 100% acetone (Nacalai Tesque, Inc.) for 1 min at room temperature, washed twice with PBS for 5 min, and blocked with 2% newborn calf serum (NCS; Equitech-Bio, Kerrville, TX, USA) in PBS for 30 min at room temperature in an incubation chamber. Sections were stained with peanut agglutinin (PNA)-biotin (dilution, 1:100; Vector Laboratories, Burlingame, CA, USA) and purified rat anti-mouse B220 (1:100; RA3-6B2, BioLegend, San Diego, CA, USA) in sterile PBS containing 2% NCS overnight at 4°C in the incubation chamber. After incubation, sections were washed with PBS containing 0.1% Tween 20 and PBS for 5 min each and stained with AF488–goat anti-rat IgG (1:200; Thermo Fisher Scientific) and AF546-streptavidin (1:200; Thermo Fisher Scientific) in sterile PBS containing 2% NCS for 30 min at room temperature in the incubation chamber. After two 5-min washes with PBS, sections were stained with 1 μM 4′,6-diamidino-2-phenylindole (DAPI) (AAT Bioquest, Sunnyvale, CA, USA) for 10 min at room temperature in an incubation chamber. Finally, sections were washed in PBS for 5 min twice, mounted in Fluoromount (Diagnostic BioSystems, Pleasanton, CA, USA), and covered with a cover glass (Matsunami Glass USA, Bellingham, WA, USA). Sections were examined under a fluorescence microscope (BZ-X800; Keyence, Osaka, Japan).

Enzyme-linked immunosorbent assay

Flat-bottom 96-well immunoplates (Thermo Fisher Scientific, Waltham, MA, USA) were coated with 1 mg/ml of OVA diluted in PBS at 4°C overnight. After incubation, the plates were blocked with 1% (w/v) bovine serum albumin (BSA; Nacalai Tesque) in PBS for 2 h at room temperature. After blocking, the plates were washed three times with PBS containing 0.05% (v/v) Tween 20 (Nacalai Tesque). Samples were serially diluted with PBS containing 1% (w/v) bovine serum albumin (BSA) and 0.05% (v/v) Tween 20, added to the plates, and

incubated for 2 h at room temperature. Plates were washed three times with PBS containing 0.05% and then incubated for 1 h at room temperature with horseradish peroxidase-conjugated goat anti-mouse IgG or IgA (Southern Biotech, Birmingham, AL, USA) diluted in PBS containing 1% (w/v) BSA and 0.05% (v/v) Tween 20. Plates were washed three times with PBS containing 0.05% Tween 20 and then incubated for 2 min at room temperature with tetramethylbenzidine peroxidase substrate (SeraCare Life Sciences, Milford, MA, USA); reactions were stopped by adding 0.5 N HCl (Nacalai Tesque). Absorbance at 450 nm was measured by using an iMark Microplate Absorbance Reader (Bio-Rad Laboratories, Hercules, CA, USA).

Cell isolation and sorting

At 24 h after nasal or subcutaneous administration of mice with 1 μg of ALA or MPLA, nasal and skin tissues were collected as previously described (24–26). The nasal septum was dissected from the skull and was treated with 2 mg/ml of collagenase for 60 min at 37°C and then filtered through a cell strainer. The skin was harvested from the injection area and the area was calculated by using graph paper. The skin samples were treated with 2 mg/ml of collagenase for 60 min at 37°C and then filtered through a cell strainer. The separated cells were used for flow cytometric analysis.

For the evaluation with antibodies to chemokines, 1 μg of ALA or MPLA with or without 2 μg of anti-CCL2 (polyclone; Abcam), 2 μg of anti-CCL3 (polyclone; Invitrogen), or 4 μg of anti-CCL4 (clone W15194A; BioLegend) was administered intranasally. After 24 h, nasal tissue was collected and treated as described earlier for flow cytometric analysis.

For sorting, cells were stained with 5 μg/ml anti-CD16/32 antibody and 7-AAD Viability Staining Solution (BioLegend, San Diego, CA, USA) for 15 min at room temperature; stained with BV421–anti-CD11c (clone N418; BioLegend), FITC–anti-EpCAM (clone G8.8; BioLegend), and APC–anti-CD45 (clone I3/2.3; BioLegend) for 30 min on ice; and sorted by using a FACSAria III (Becton Dickenson, Franklin Lakes, NJ, USA). The sorted cells were used for quantitative polymerase chain reaction (qPCR) analysis.

Quantitative polymerase chain reaction

Gene expression analysis of cytokines and chemokines involved reverse transcription as described previously (27) and qPCR assay according to the manufacturer's instructions (Bio-Rad). RNA was extracted from sorted cells by using Sepasol-RNA I Super G (Nacalai Tesque) and chloroform (Nacalai Tesque), precipitated with 2-propanol (Nacalai Tesque), and washed with 75% (vol/vol) ethanol (Nacalai Tesque). RNA samples were then incubated with DNase I (Invitrogen, Carlsbad, CA, USA) to remove contaminating genomic DNA and reverse-transcribed into cDNA (Superscript III reverse transcriptase, VIRO cDNA Synthesis Kit, Invitrogen). qPCR analysis was performed on a CFX Opus 96 thermocycler (Bio-Rad) by using SsoAdvanced Universal Probes Supermix and PrimePCR *Gapdh*, *Tlr4*, *Csf2*, *Ccl2*, *Ccl3*, and *Ccl4* primers for mice with FAM probe (Bio-Rad) according to the manufacturer's protocol.

Flow cytometric analysis

Cells were stained with 5 μg/ml anti-CD16/32 antibody (Fc Block, clone 93; BioLegend) and 7-AAD Viability Staining Solution (BioLegend) for 15 min at room temperature.

For the examination of cDCs, cells were then stained with BV421–anti-CD11c (clone N418; BioLegend), FITC–anti-I-A^d (clone AMS-32.1; Becton Dickenson), PE–anti-CD103 (clone M290; Becton Dickenson), PE–Cy7–anti-CD40 (clone 3/23; BioLegend), PE-Cy7–streptavidin (Becton Dickenson), APC–anti-CD11b (clone M1/70; BioLegend), APC-Cy7–anti-CD8α (clone 53-6.7; BioLegend), biotin–anti-CD80 (clone 16-10A1; Becton Dickenson), and biotin–anti-CD86 (clone GL-1; Becton Dickenson) for 30 min on ice.

To assess cDC2As and cDC2Bs, cells were stained with BV421–anti-CD11c (clone N418; BioLegend), FITC–anti-I-A^d (clone AMS-32.1; Becton Dickenson), PE–anti-CD103 (clone M290; Becton Dickenson), APC–anti-CLEC10A (CD301, clone LOM-14; BioLegend), and APC-Cy7–CD11b (clone M1/70; BioLegend) for 30 min on ice. To examine GC B cells, cells were stained with BV421–anti-B220 (clone RA3-6B2; BioLegend), FITC–anti-IgA (clone C10-3, Becton Dickenson), PE–anti-CD3ε (clone 145-2C11; Becton Dickenson), AF647–anti-GL7 (clone GL7; BioLegend) for 30 min on ice. To evaluate T_{fh} cells, cells were then stained with BV421–anti-CD4 (clone RM4-5; BioLegend), FITC–anti-CD3ε (clone 145-2C11; Becton Dickenson), PE–anti-PD-1 (clone 29F.1A12; BioLegend), PE-Cy7–anti-CD8α (clone 53-6.7; BioLegend) for 30 min on ice. Stained cells then underwent flow cytometry (MACSQuant, Miltenyi Biotec, Bergish Gladbach, Germany).

Statistics

All statistical analyses were performed by using PRISM 6 software (GraphPad Software, San Diego, CA, USA). Data are shown as mean ± 1 SD. Differences between ALA, MPLA, and Mock groups were analyzed by one-way analysis of variance (ANOVA) followed by Tukey's multiple-comparisons test. $P < .05$ was considered significant.

Results

ALA showed superior adjuvant activity in nasal immunization in mice

We previously demonstrated that ALA is an effective adjuvant for subcutaneous and nasal vaccination (19, 20). Here, we compared the adjuvanticity of ALA with that of a licensed adjuvant, MPLA, in mice for both nasal and subcutaneous vaccines. In subcutaneous immunization, ALA induced higher levels of OVA-specific IgG in serum than did MPLA (Fig. 1A); although the differences between ALA and MPLA were statistically significant, they were not clinically relevant.

In contrast, the nasal wash, bronchoalveolar lavage fluid, and serum of mice nasal immunized with OVA plus ALA all contained high levels of OVA-specific IgA antibody, whereas only scant responses were induced in the Mock and MPLA groups (Fig. 1B and Supplementary Fig. S1). Furthermore, ALA also induced serum OVA-specific IgG antibodies, and these levels were higher than those in the Mock and MPLA groups (Fig. 1C). These results indicate that ALA was superior to MPLA as a mucosal adjuvant in nasal immunization.

ALA enhances germinal center formation in nasal immunization

Efficient nasal immunity is associated with the generation of germinal centers (GCs) in NALT and CLNs (28). The secretion of IgA is due to IgA class switching of B cells supported by the T_{fh} cells in GCs (29). Immunohistological analysis of the nasally immunized mice revealed more GCs in the NALT of the ALA group than the MPLA and Mock groups (Fig. 2A and Supplementary Fig. S2). Consistent with these results, the percentages of both GC GL7^{hi} B cells and IgA^{+} GL7^{hi} B cells among total B cells were increased in the NALT of the ALA group compared with the Mock and MPLA groups (Fig. 2B and Supplementary Fig. S3A–B). In addition, the percentage of PD-1^{hi} T_{fh} cells among total T cells in NALT was greater in the ALA group than in the Mock and MPLA groups (Fig. 2C and Supplementary Fig. S3C). These results

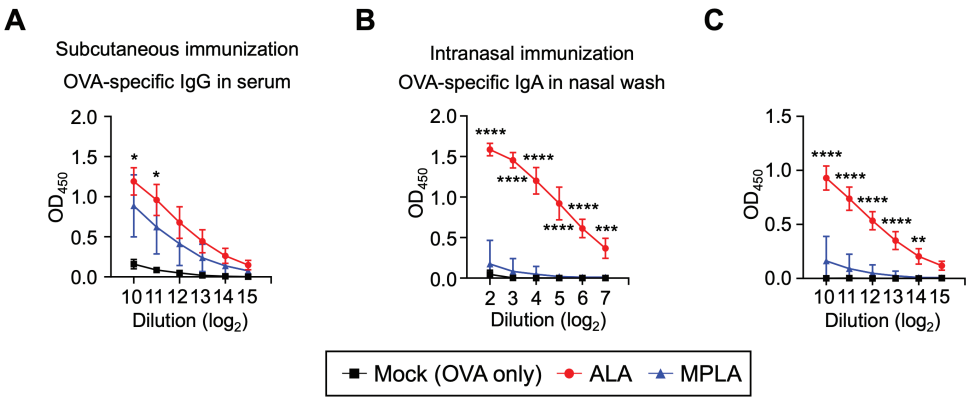

Figure 1. For both intranasal and subcutaneous vaccination, *Alcaligenes*-derived lipid A (ALA) induced higher levels of antigen-specific antibodies than did monophosphoryl lipid A (MPLA). In particular, ALA was superior for intranasal vaccination. (A) OVA-specific IgG in the serum of mice vaccinated subcutaneously was evaluated by ELISA ($n = 4$). (B) OVA-specific IgA in the nasal wash of mice vaccinated intranasally was evaluated by ELISA ($n = 4$). (C) OVA-specific IgG in the serum of mice vaccinated intranasally was evaluated by ELISA ($n = 4$). The data are shown as the mean ± 1 SD from two independent experiments; differences were analyzed by two-way analysis of variance (ANOVA; $^{*}P < .05$, $^{**}P < .01$, $^{***}P < .001$, $^{****}P < .0001$)..

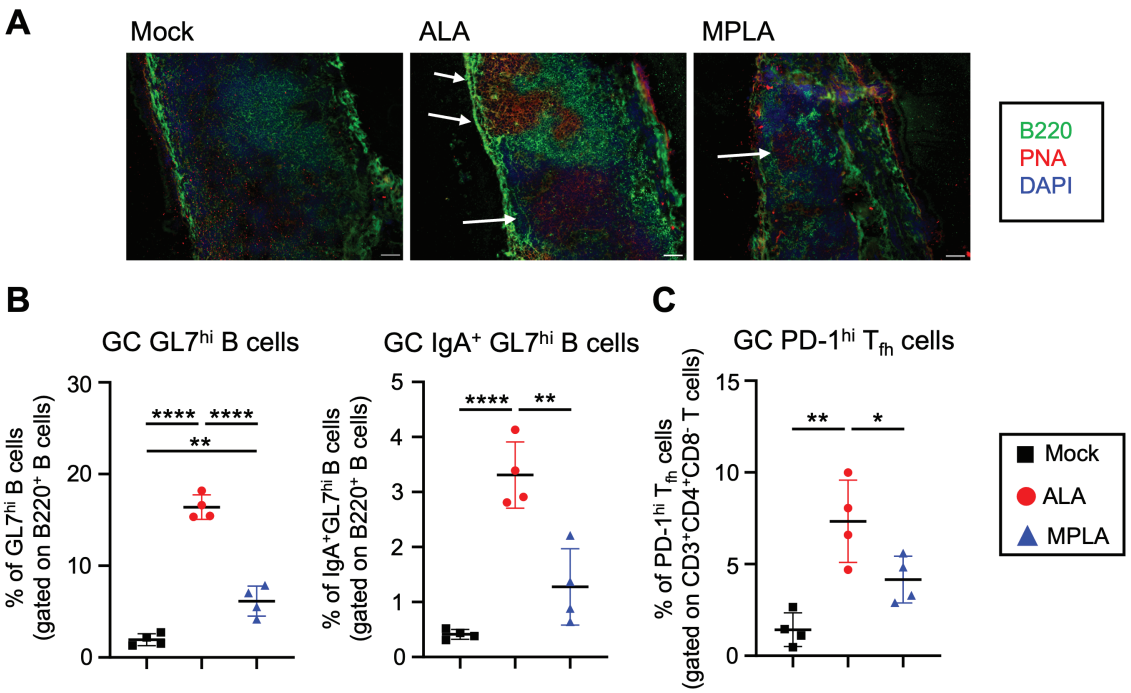

Figure 2. Intranasal administration of ALA increased the generation of GCs and the numbers of GC B cells, IgA^{+} GL7^{hi} B cells, and T_{fh} cells in NALT. (A) GCs (arrows) in NALT were analyzed through immunohistochemistry. PNA: GC marker; B220: B cell marker ($n = 4$) (scale bar = 200 μm). (B) The populations of GC GL7^{hi} B cells (gated on: CD3ε^{-} B220^{+} GL7^{hi}) and IgA^{+} GL7^{hi} B cells (gated on: CD3ε^{-} B220^{+} GL7^{hi} IgA^{+}) in NALT were analyzed by flow cytometry ($n = 4$). (C) The population of T_{fh} cells (gated on: CD3ε^{+} CD8α^{-} CD4^{+} PD-1^{hi}) in NALT was analyzed by flow cytometry ($n = 4$). The data are shown as the mean ± 1 SD from two independent experiments; differences were analyzed by one-way ANOVA ($^{*}P < .05$, $^{**}P < .01$, $^{****}P < .0001$).

demonstrate that ALA promoted the generation of GC in NALT, with an increase in GC GL7^{hi} B cells, especially IgA^{+} GL7^{hi} B cells, and PD-1^{hi} T$_{fh}$ cells, to induce the production of IgA in the nose.

We also performed similar studies on the CLNs, which are the draining lymph nodes during nasal immunity. Similar to the findings for NALT, the generation of GCs, percentages of GL7^{hi} B cells, IgA^{+} GL7^{hi} B cells, and PD-1^{hi} T$_{fh}$ cells in the CLNs were greater in the ALA group than in the Mock and MPLA groups (Fig. 3, Supplementary Figs. S4 and S5). These results suggested that nasal vaccination with ALA-induced GC generation in CLNs and increased the populations of GC GL7^{hi} B cells, PD-1^{hi} T$_{fh}$ cells, and IgA^{+} GL7^{hi} B cells for subsequent systemic immunity.

ALA promoted the infiltration and activation of CD11b^{+} CD103^{-} CD11c^{+} DCs in nasal tissue

We previously reported that ALA exerted adjuvant activity through the activation of DCs (19). Therefore, we compared the effects of ALA and MPLA on DCs to understand the mechanism underlying ALA's superiority as a nasal vaccine adjuvant. We detected more CD11b^{+} CD103^{-} CD11c^{+} MHC II^{+} cells, which are defined as subtype 2 conventional DCs (cDC2s), in nasal tissue after the nasal administration of ALA than of MPLA (Fig. 4A and Supplementary Fig. S6A). In contrast, ALA did not affect the number of CD103^{+} CD11b^{-} CD11c^{+} MHC II^{+} cells, which are considered as cDC1s, and these cell counts were similar among the ALA, MPLA, and Mock groups (Fig. 4A and Supplementary Fig. S6A). In addition, the cell densities of both cDC1s and cDC2s in the skin were similar after subcutaneous administration of either ALA or MPLA (Fig. 4B and Supplementary Fig. S6B).

Moreover, cDC2s can be further divided into cDC2A and cDC2B subtypes, which have different functions during immunity (30). We used C-type lectin domain family 10 member A (CLEC10A, CD301) as a marker to differentiate cDC2As and cDC2Bs. Compared with cell counts in the Mock group, intranasal administration of lipid A increased the population of cDC2As (Fig. 4C). In addition, the cDC2A population was larger after treatment with ALA than with MPLA (Fig. 4C).

Next, we assessed the activation of DCs according to the expression levels of co-stimulatory molecules (CD40, CD80, and CD86) after intranasal administration with ALA or MPLA. The expression of CD40 and CD80 was upregulated on CD11b^{+} CD103^{-} CD11c^{+} cells in the ALA group, and these levels were higher than those in the MPLA group (Fig. 5A and B), but both groups had little change in the expression of CD86 (Supplementary Fig. S7A). After subcutaneous administration of adjuvant, only the expression of CD40 was upregulated after stimulation by ALA or MPLA; these levels were similar between adjuvants, and neither ALA nor MPLA increased CD80 or CD86 expression (Supplementary Fig. S7B–D). These results demonstrate that intranasally administered ALA promoted greater infiltration and activation of CD11b^{+} CD103^{-} CD11c^{+} DCs in nasal tissue than did MPLA.

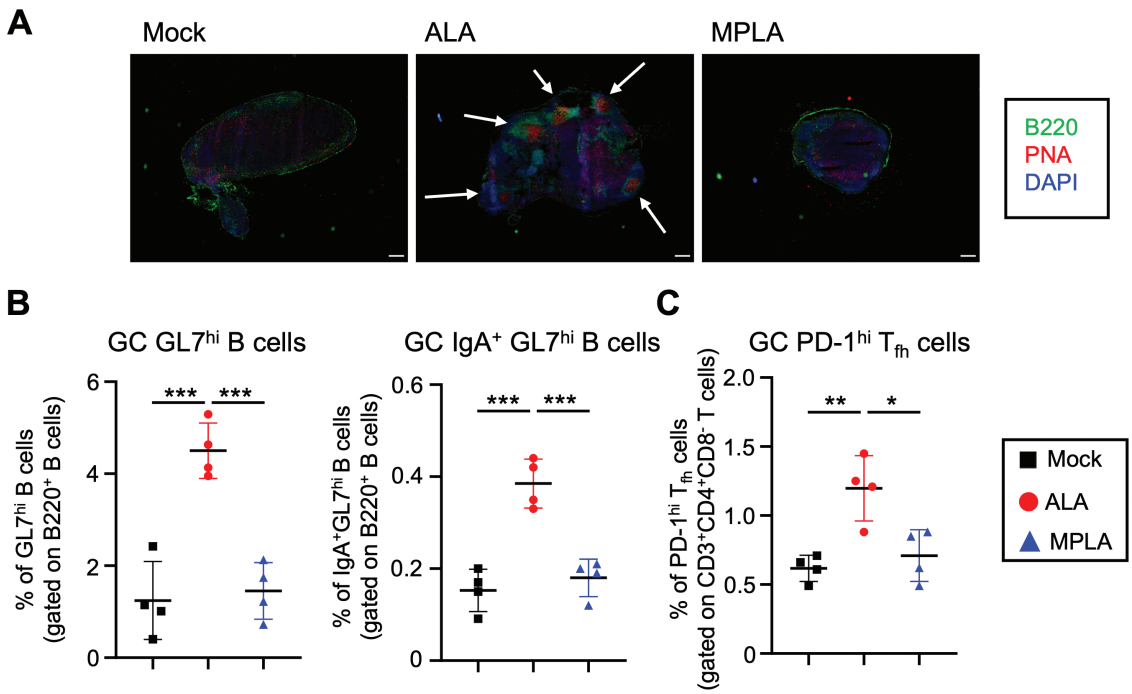

Figure 3. Intranasal administration of ALA increased the generation of GCs and the numbers of GC B cells, IgA^{+} GL7^{hi} B cells, and T$_{fh}$ cells in CLNs. (A) GCs (arrows) in CLNs were analyzed by immunohistochemistry. PNA: GC marker; B220: B cell marker (n = 4) (scale bar = 50 μm). (B) The populations of GC GL7^{hi} B cells (gated on: CD3ε^{-} B220^{+} GL7^{hi}) and IgA^{+} GL7^{hi} B cells (gated on: CD3ε^{-} B220^{+} GL7^{hi} IgA^{+}) in CLNs were analyzed by flow cytometry (n = 4). (C) The population of T$_{fh}$ (gated on: CD3ε^{+} CD8α^{-} CD4^{+} PD-1^{hi}) in CLNs was analyzed by flow cytometry (n = 4). The data are shown as the mean ± 1 SD from two independent experiments; differences were analyzed by one-way ANOVA (*P < .05, **P < .01, ***P < .001).

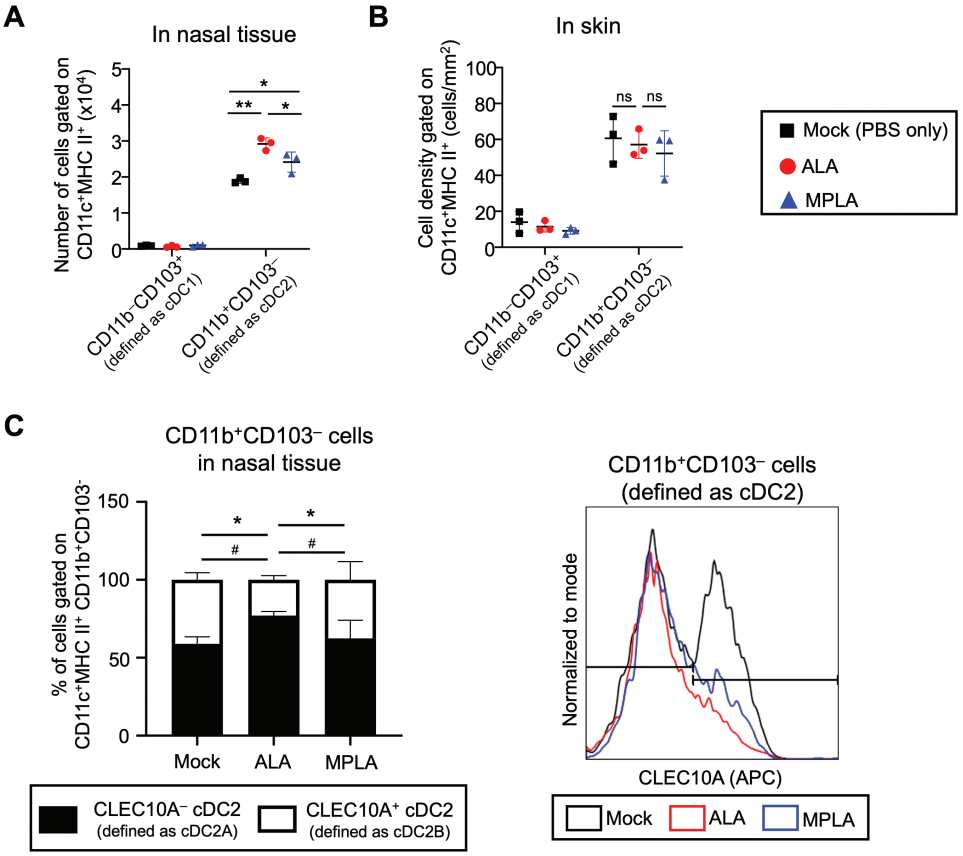

Figure 4. Intranasal administration of ALA induced greater infiltration of type 2 conventional DCs (cDC2s) in nasal tissue than did MPLA. (A) The numbers of CD103⁺ CD11b⁻ cDC1s and CD11b⁺ CD103⁻ cDC2s due to intranasal adjuvant administration were evaluated by flow cytometry ($n = 3$). (B) The density of CD103⁺ CD11b⁻ cDC1s and CD11b⁺ CD103⁻ cDC2s due to subcutaneous adjuvant administration were evaluated by flow cytometry ($n = 3$). (C) The populations of CD11b⁺ CD103⁻ CLEC10A⁻ cDC2As (*) and CD11b⁺ CD103⁻ CLEC10A⁺ cDC2Bs (#) in nasal tissue were analyzed by flow cytometry ($n = 4$). The data are shown as the mean ± 1 SD from two independent experiments; differences were analyzed by one-way ANOVA (*,#$P < .05$, **$P < .01$; ns, not significant).

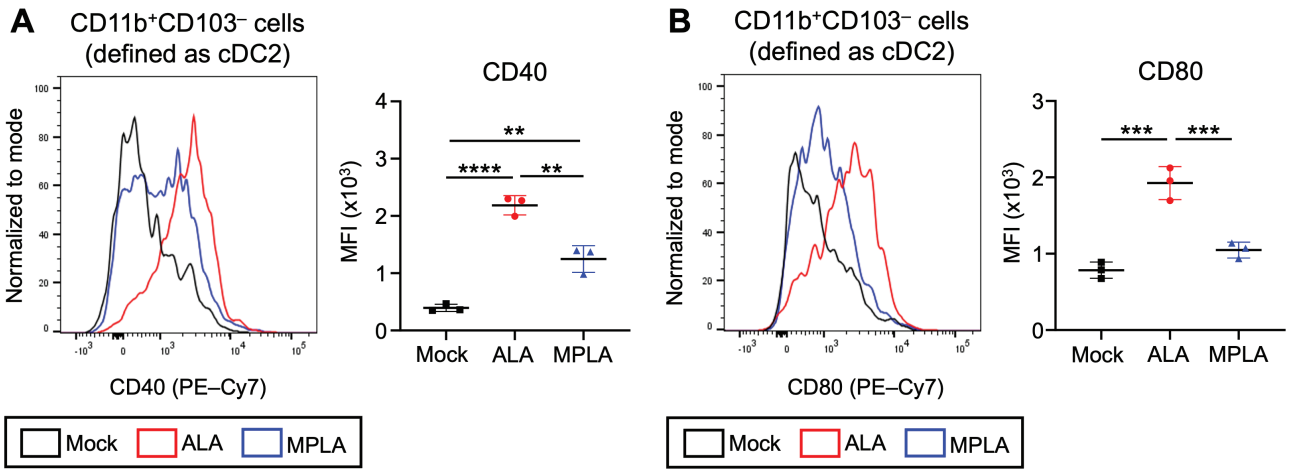

Figure 5. Intranasally administered ALA induced greater expression of CD40 and CD80 than did MPLA. The expression of (A) CD40 and (B) CD80 on cDC2s after intranasal adjuvant administration was evaluated by flow cytometry ($n = 3$). The data are shown as the mean ± 1 SD from two independent experiments; differences were analyzed by one-way ANOVA (**$P < .01$, ***$P < .001$, ****$P < .0001$).

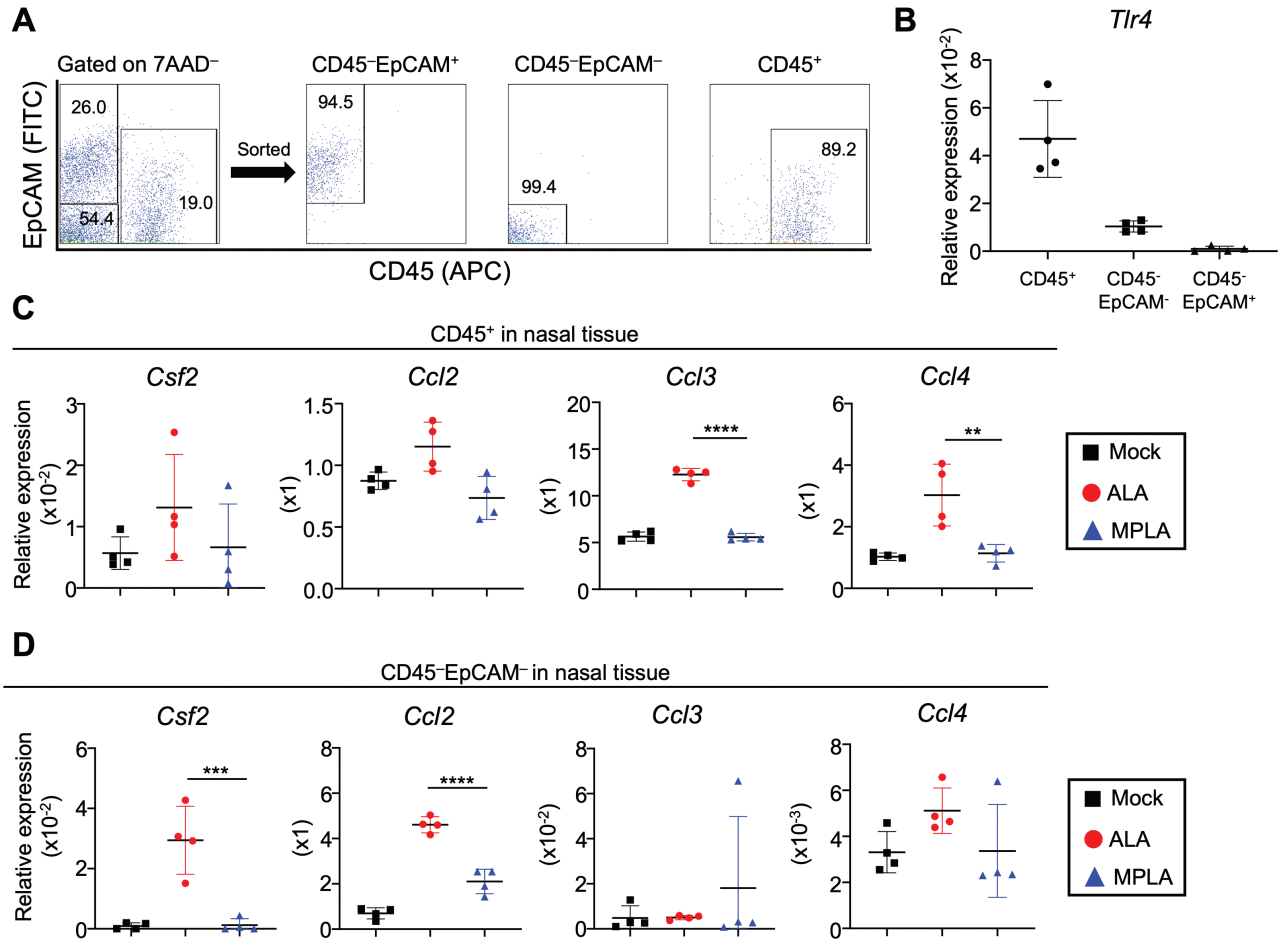

Figure 6. The gene expression of *Csf2*, *Ccl2*, *Ccl3*, *Ccl4*, and *Tlr4* in sorted cells from nasal tissue. (A) The sorting strategy for CD45⁺ immune cells, EpCAM⁺ CD45⁻ epithelial cells, and double-negative stromal cells ($n = 4$). (B) The gene expression of *Tlr4* on sorted cells was evaluated by quantitative PCR (qPCR) analysis ($n = 4$). (C) The gene expression of *Csf2*, *Ccl2*, *Ccl3*, and *Ccl4* from CD45⁺ cells due to stimulation by ALA or MPLA was evaluated by qPCR ($n = 4$). (D) The gene expression of *Csf2*, *Ccl2*, *Ccl3*, and *Ccl4* from double-negative cells due to stimulation by ALA or MPLA was evaluated by qPCR ($n = 4$). The data are shown as the mean ± 1 SD from two independent experiments; differences were analyzed by one-way ANOVA (**$P < .01$, ***$P < .001$, ****$P < .0001$).

ALA elevated the expression of CCL2 on stromal cells and of CCL3 and CCL4 on CD45⁺ immune cells in nasal tissue

In the nasal mucosa, various hematopoietic cells (i.e. immune cells), and non-hematopoietic cells (e.g. epithelial cells, stromal cells) play important roles in the regulation of immune responses, including the recruitment and activation of DCs (31). To verify the cells targeted by ALA, we sorted cells from nasal tissue according to their expression of CD45 and epithelial cell adhesion molecule (EpCAM) (Fig. 6A) and examined the subpopulations' expression of TLR4, a receptor for ALA (22, 32). We found that CD45⁺ immune cells showed the greatest gene expression of *Tlr4* (Fig. 6B). Among CD45⁻ non-hematopoietic cells, EpCAM⁻ stromal cells—but not EpCAM⁺ epithelial cells—moderately expressed the *Tlr4* gene (Fig. 6B). These results suggest that ALA may affect CD45⁺ immune cells and CD45⁻ EpCAM⁻ stromal cells.

Chemokines (e.g. CCL2, 3, 4) and GM-CSF are considered key factors for recruiting DCs and stimulating their proliferation (33–35). Consistent with its effects on TLR4 expression, ALA upregulated the expression of *Ccl3* and *Ccl4* on CD45⁺ immune cells (Fig. 6C), whereas *Ccl2* expression was preferentially increased on stromal cells (Fig. 6D). Moreover, ALA increased the expression of *Csf2* (encoding GM-CSF) on stromal cells but not on CD45⁺ immune cells (Fig. 6D). In addition, epithelial cells showed almost no response to either ALA or MPLA (Supplementary Fig. S8). These results indicate that ALA induced the gene expression of *Ccl2* and *Csf2* on stromal cells and of *Ccl3* and *Ccl4* on CD45⁺ immune cells from nasal tissue; these chemokine responses likely promoted the infiltration of cDC2s into nasal tissue.

To investigate which chemokine is critical for recruiting cDC2s into nasal tissue, we nasally co-administered ALA with either anti-CCL2, anti-CCL3, or anti-CCL4 antibody. We found that the infiltration of cDC2s induced by ALA in nasal tissue was significantly inhibited by the anti-CCL2 and anti-CCL3 antibodies, whereas anti-CCL4 antibody had no inhibitory

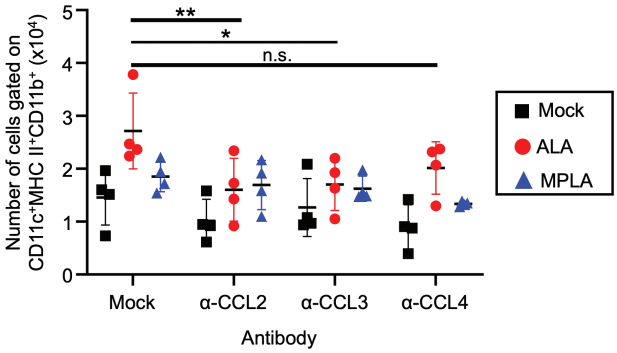

Figure 7. Intranasal administration of ALA with anti-CCL2 or anti-CCL3 antibodies inhibited the infiltration of cDC2s in nasal tissue. The numbers of $CD11b^+$ $CD103^-$ cDC2s in nasal tissue were analyzed by flow cytometry ($n = 4$). The data are shown as the mean ± 1 SD from two independent experiments; differences were analyzed by two-way analysis of variance (ANOVA; $^*P < .05$, $^{**}P < .01$; ns, not significant).

effect (Fig. 7). These findings indicate that CCL2 and CCL3 are critical chemokines for the ALA-initiated recruitment of cDC2s into the nasal tissue.

Discussion

In this study, we compared the adjuvant activity of ALA and MPLA and demonstrated the superiority of ALA as a nasal vaccine adjuvant. In intranasal vaccination, ALA increased the number of cDC2s in nasal tissue by upregulating their expression of chemokines; these activated cDC2s, thus showing increased expression of co-stimulatory molecules. In contrast, MPLA lacked these effects. Together, these findings imply that ALA is suitable as an intranasal vaccine adjuvant.

The structure of lipid A informs its ability to activate TLR4 signaling. In particular, phosphoryl groups influence the binding of lipid A to TLR4 (36). Compared with the two phosphoryl groups of ALA (23), MPLA is dephosphorylated and exists in a monophosphorylated form (37). The presence of a single phosphoryl group instead of two hampers dimerization of the TLR4–MD-2 complex, thus altering its downstream signaling pathways and the subsequent immune responses of antigen-presenting cells such as DCs (38, 39). The structural uniqueness of ALA may underlie the differences in immune responses compared with those from MPLA.

In the studies of GCs in NALT and CLNs, the promotion of GC generation and the populations of GC B cells, especially IgA^+ $GL7^{hi}$ B cells, and T_{fh} cells by intranasal vaccination with ALA was consistent with the production of nasal and systemic IgA. Mucosal immunity and class switching to IgA^+ B cells are dependent on Th17 cells. In our previous reports, the stimulation of DCs with ALA stimulated the production of IL-6 and IL-23 and, consequently, enhanced the differentiation of Th17 cells from naive T cells (19, 20, 32). These results suggest that ALA is suitable for use as a nasal vaccine adjuvant.

To further investigate the underlying mechanism, we focused on DCs, which are the starting point for the generation of GCs (40). Our results suggest that the ALA-induced increase in the number of activated cDC2s in nasal tissue may have been responsible for the superiority of ALA in nasal vaccination. As previously shown, cDC2s are a key component in the process of mucosal immunity (41). Compared with other types of DCs, cDC2s—because of their expression of MHC II—show specialized antigen presentation and greater induction of $CD4^+$ T-cell proliferation (42). Furthermore, cDC2s reportedly are more suitable for presenting soluble antigens than for presenting particle antigens (43). These properties of cDC2s imply that these cells are indispensable in the generation of mucosal immunity. Moreover, ALA-induced cDC2s expressed higher levels of CD40 and CD80 than those exposed to MPLA; these co-stimulatory molecules play important roles in the activation and differentiation of T cells. In a previous study, the expression of CD80 from DCs increased the activation of T cells overall (44), whereas the expression of CD40 from DCs upregulated the differentiation of Th17 cells (45). In our previous report, ALA induced greater production of IL-6 and IL-23 than did MPLA, subsequently leading to increased differentiation of Th17 cells (32). Because the Th17 response is indispensable in the generation of mucosal immunity and secretion of IgA (46, 47), the robust ALA-associated Th17 response may explain the superiority of ALA in intranasal immunity. Taken together, the superiority of ALA in mucosal immunity was strongly related to ALA's ability to promote the infiltration and activation of cDC2s.

However, in subcutaneous vaccines, ALA and MPLA had similar effects. One possible reason is the regulatory effect of subcutaneous adipose tissue on ALA-induced inflammatory activity. In subcutaneous administration, vaccines are injected into the subcutaneous adipose tissue, which contains not only adipocytes but also endothelial cells, fibroblasts, stem cells, and immune cells (48). These immune cells include M2 macrophages and Tregs, which usually suppress inflammation in a healthy host (49). Adipose tissue is a key source of IL-10, and LPS stimulation of adipose tissue increases IL-10 levels (50). Overall, the anti-inflammatory homeostatic effect of adipose tissue in healthy hosts may explain the similar cDC activation profiles of ALA and MPLA (Supplementary Fig. S7B–D).

In contrast, stimulation with ALA did not alter DC populations in the skin. In a previous report, DCs that infiltrated into adipose tissue proliferated only in the context of chronic inflammation, such as obesity (51). However, the inflammation induced by vaccines is more similar to acute inflammation than to chronic inflammation (52). These studies show the tendency of adipose tissue to maintain homeostasis and prevent inflammation in healthy hosts. This tendency may explain the low activation state of cDC2s, their consistent number, and their limited secretion of IgG after subcutaneous administration of ALA. As another possibility, sensitivity toward OVA was markedly stronger in subcutaneous than intranasal administration. The stimulation due to OVA might overwhelm the activity of ALA. In a previous review, the immunogenicity of vaccines was significantly improved through intramuscular

administration compared with subcutaneous administration, particularly in terms of the antibody response and seroconversion of intramuscularly administered adjuvanted vaccines (53). Further discussions regarding the optimal administration route of ALA are warranted.

cDC2s can be categorized as cDC2As and cDC2Bs according to the expression of several markers (e.g. CLEC4A, CLEC10A, CLEC12A, ESAM) (54). We found that cDC2As were increased within nasal tissue in the ALA group. Although additional studies are required, ALA's high antigen presentation activity, induction of T cells, and induction of chemokine production (i.e. CCL3 and CCL4) in cDC2As (54), which are superior to cDC2Bs, may explain at least partially the adjuvant activity of ALA.

Regarding the increase of cDC2s in nasal tissue, the mechanisms underlying the recruitment of DCs from the bone marrow and their circulation into immunization sites are still not well understood (55). In some previous studies, pre-cDCs expressed CCR2, the receptor of CCL2, thus allowing pre-cDCs to migrate from the bone marrow to the periphery through interaction with CCL2 (56). Moreover, both CCR1 and CCR5 can recognize CCL3 (57), and CCL4 can bind to CCR5 (58). cDCs express these receptors, which when bound by chemokines, induce their recruitment and migration (35). In our current study, only cDC2s—not cDC1s—accumulated in nasal tissue. Although ALA seems to recruit cDC2s specifically, the mechanism underlying this effect is unclear.

In this study, we noted that the source of CCL2 was stromal cells. In previous studies, pulmonary stromal cells appeared to modulate the response to LPS or house dust mite allergen, which can recruit and activate innate immune cells such as DCs (59). Other studies showed that the CCL2 secreted by stromal cells promotes antibacterial defense (60). In contrast, we found that the source of CCL3 and CCL4 was $CD45^+$ immune cells. Candidates for the specific cell types include DCs themselves, which secrete CCL3 and CCL4 after stimulation with LPS (61). These findings imply that the complex cell interaction initiated through ALA induces chemokine responses in nasal immunization. In addition, GM-CSF can promote the differentiation of cDCs from pre-cDCs (34) and the proliferation of myeloid-lineage cells (33). Moreover, stimulation by GM-CSF is indispensable in the development of monocyte-derived DCs (62), which show a similar phenotype and function to cDC2s. Thus, the effects of ALA on stromal cells and $CD45^+$ immune cells contribute markedly to mucosal immunity.

In conclusion, after both intranasal and subcutaneous administration, ALA induced higher levels of antigen-specific antibody secretion than did MPLA. In particular, ALA was superior in intranasal vaccination. Consistent with its effects on nasal and systemic IgA production, ALA promoted the generation of GCs in NALT and CLNs and increased the populations of GC B cells, IgA^+ B cells, and T_{fh} cells. As the possible mechanism underlying the superiority of ALA in nasal vaccines, ALA promoted the infiltration of highly activated $CD11b^+$ cDC2s in nasal tissue and, in particular, increased cDC2A cell counts. In addition, ALA induced the expression of GM-CSF and CCL2 on stromal cells and CCL3 and CCL4 on $CD45^+$ immune cells in nasal tissue; among these chemokines, CCL2 and CCL3 helped to recruit cDC2s into nasal tissue.

Conflict of interest statement. None declareds.

Funding

This study was supported by the Japan Society for the Promotion of Science KAKENHI (grant numbers 21H02757, 20H05697, 20H04117, 20K08534, and 21H02145 to JK; 22K15004 to KH; 15H05836, 16H01885, 20H00404, and 20H05675 to KF; 18H04620, 20H04776, and 20K05727 to A. Shimoyama; 22KJ2175 to KY; and 22J12595 to HY); Japan Science and Technology Agency CREST (grant number JPMJCR20R3 to KF); Japan Agency for Medical Research and Development (grant numbers 22fk0108145h0003, 22ae0121042h0002, 22ae0121035s0102, and 223fa727001h0001 to JK; 20ek0109444h0001 and 21ek0109444h0002 to KF; and 223fa727001s0301 to A. Shimoyama); Ministry of Health, Labour and Welfare of Japan and Public/Private R&D Investment Strategic Expansion Program: PRISM (grant number 20AC5004 to JK); Cross-ministerial Strategic Innovation Promotion Program: SIP (grant number 18087292 to JK); Grant for Joint Research Project of the Institute of Medical Science, The University of Tokyo (to JK); Ono Medical Research Foundation (to JK); Canon Foundation (to JK); Osaka University Foundation for the Future (COVID-19 Response Fund, to KF); Multidisciplinary PhD program for Pioneering Quantum Beam Application (to HY); and Quantum LEAder Resource (to HY).

References

1. Ols S, Yang L, Thompson EA, *et al*. Route of vaccine administration alters antigen trafficking but not innate or adaptive immunity. *Cell Rep* 2020;**30**:3964–3971.e7. https://doi.org/10.1016/j.celrep.2020.02.111
2. Tang DCC, Nguyen HH. The Yin-Yang arms of vaccines: disease-fighting power versus tissue-destructive inflammation. *Expert Rev Vaccines* 2014;**13**:417–27. https://doi.org/10.1586/14760584.2014.882775
3. Zhang L, Wang W, Wang S. Effect of vaccine administration modality on immunogenicity and efficacy. *Expert Rev Vaccines* 2015;**14**:1509–23. https://doi.org/10.1586/14760584.2015.1081067
4. Calzas C, Chevalier C. Innovative mucosal vaccine formulations against influenza a virus infections. *Front Immunol* 2019;**10**:1–21.
5. Afkhami S, D'Agostino MR, Zhang A, *et al*. Respiratory mucosal delivery of next-generation COVID-19 vaccine provides robust protection against both ancestral and variant strains of SARS-CoV-2. *Cell* 2022;**185**:896–915.e19. https://doi.org/10.1016/j.cell.2022.02.005
6. Kozlowski PA, Aldovini A. Mucosal vaccine approaches for prevention of HIV and SIV transmission. *Curr Immunol Rev* 2018;**15**:102–22. https://doi.org/10.2174/1573395514666180605092054
7. Lavelle EC, Ward RW. Mucosal vaccines—fortifying the frontiers. *Nat Rev Immunol* 2022;**22**:236–50. https://doi.org/10.1038/s41577-021-00583-2
8. Alu A, Chen L, Lei H, *et al*. Intranasal COVID-19 vaccines: from bench to bed. *eBioMedicine* 2022;**76**:103841. https://doi.org/10.1016/j.ebiom.2022.103841
9. Luria-Pérez R, Sánchez-Vargas LA, Muñoz-López P, *et al*. Mucosal vaccination: a promising alternative against flaviviruses. *Front Cell Infect Microbiol* 2022;**12**:1–20.
10. Ho NI, Huis In 't Veld LGM, Raaijmakers TK, *et al*. Adjuvants enhancing cross-presentation by dendritic cells: the key to more effective vaccines? *Front Immunol* 2018;**9**:2874. https://doi.org/10.3389/fimmu.2018.02874
11. Miyaji EN, Carvalho E, Oliveira MLS, *et al*. Trends in adjuvant development for vaccines: DAMPs and PAMPs as potential new adjuvants. *Braz J Med Biol Res Revista brasileira de pesquisas medicas e biologicas* 2011;**44**:500–13. https://doi.org/10.1590/s0100-879x2011007500064

12. Monie A, Hung CF, Roden R, *et al*. Cervarix™: a vaccine for the prevention of HPV 16, 18-associated cervical cancer. *Biol Targets Ther* 2008;**2**:107–13.
13. Mitchell TC, Casella CR. No pain no gain? Adjuvant effects of alum and monophosphoryl lipid A in pertussis and HPV vaccines. *Curr Opin Immunol* 2017;**47**:17–25. https://doi.org/10.1016/j.coi.2017.06.009
14. Ismaili J, Rennesson J, Aksoy E, *et al*. Monophosphoryl lipid A activates both human dendritic cells and T cells. *J Immunol (Baltimore, Md.: 1950)* 2002;**168**:926–32.
15. ten Brinke A, Karsten ML, Dieker MC, *et al*. The clinical grade maturation cocktail monophosphoryl lipid A plus IFNγ generates monocyte-derived dendritic cells with the capacity to migrate and induce Th1 polarization. *Vaccine* 2007;**25**:7145–52. https://doi.org/10.1016/j.vaccine.2007.07.031
16. Thompson BS, Chilton PM, Ward JR, *et al*. The low-toxicity versions of LPS, MPL(R) adjuvant and RC529, are efficient adjuvants for CD4+ T cells. *J Leukoc Biol* 2005;**78**:1273–80. https://doi.org/10.1189/jlb.0305172
17. Obata T, Goto Y, Kunisawa J, *et al*. Indigenous opportunistic bacteria inhabit mammalian gut-associated lymphoid tissues and share a mucosal antibody-mediated symbiosis. *Proc Natl Acad Sci USA* 2010;**107**:7419–24. https://doi.org/10.1073/pnas.1001061107
18. Wang Y, Hosomi K, Shimoyama A, *et al*. Lipopolysaccharide derived from the lymphoid-resident commensal bacteria *Alcaligenes faecalis* functions as an effective nasal adjuvant to augment IgA antibody and Th17 cell responses. *Front Immunol* 2021;**12**:1–10.
19. Wang Y, Hosomi K, Shimoyama A, *et al*. Adjuvant activity of synthetic lipid a of *Alcaligenes*, a gut-associated lymphoid tissue-resident commensal bacterium, to augment antigen-specific IgG and Th17 responses in systemic vaccine. *Vaccines* 2020;**8**:395–12. https://doi.org/10.3390/vaccines8030395
20. Yoshii K, Hosomi K, Shimoyama A, *et al*. Chemically synthesized *Alcaligenes* lipid a shows a potent and safe nasal vaccine adjuvant activity for the induction of *Streptococcus pneumoniae*-specific IgA and Th17 mediated protective immunity. *Microorganisms* 2020;**8**:1102–20. https://doi.org/10.3390/microorganisms8081102
21. Liu Z, Hosomi K, Shimoyama A, *et al*. Chemically synthesized *Alcaligenes* lipid A as an adjuvant to augment immune responses to *Haemophilus influenzae* type B conjugate vaccine. *Front Pharmacol* 2021;**12**:1–9.
22. Shibata N, Kunisawa J, Hosomi K, *et al*. Lymphoid tissue-resident *Alcaligenes* LPS induces IgA production without excessive inflammatory responses via weak TLR4 agonist activity. *Mucosal Immunol* 2018;**11**:693–702. https://doi.org/10.1038/mi.2017.103
23. Shimoyama A, Di Lorenzo F, Yamaura H, *et al*. Lipopolysaccharide from gut-associated lymphoid-tissue-resident *Alcaligenes faecalis*: complete structure determination and chemical synthesis of its lipid A. *Angew Chem Int Ed Engl* 2021;**60**:10023–31. https://doi.org/10.1002/anie.202012374
24. Davidson DJ, Gray MA, Kilanowski FM, *et al*. Murine epithelial cells: isolation and culture. *J Cyst Fibros* 2004;**3**:59–62. https://doi.org/10.1016/j.jcf.2004.05.013
25. Antunes MB, Woodworth BA, Bhargave G, *et al*. Murine nasal septa for respiratory epithelial air–liquid interface cultures. *Biotechniques* 2007;**43**:195–6, 198, 200 passim. https://doi.org/10.2144/000112531
26. Galvez-Cancino F, Lopez E, Lladser A. Analysis of tissue-resident immune cells from mouse skin and lungs by flow cytometry. *Methods Mol Biol* 2019;217–22.
27. Nagatake T, Shiogama Y, Inoue A, *et al*. The 17,18-epoxyeicosatetraenoic acid–G protein coupled receptor 40 axis ameliorates contact hypersensitivity by inhibiting neutrophil mobility in mice and cynomolgus macaques. *J Allergy Clin Immunol* 2018;**142**:470–484.e12. https://doi.org/10.1016/j.jaci.2017.09.053
28. Sabirov A, Metzger DW. Intranasal vaccination of infant mice induces protective immunity in the absence of nasal-associated lymphoid tissue. *Vaccine* 2008;**26**:1566–76. https://doi.org/10.1016/j.vaccine.2008.01.027
29. Chorny A, Puga I, Cerutti A. Innate Signaling Networks in Mucosal IgA Class Switching. *Adv Immunol* 2010;**107**:31–69.
30. Shin JY, Wang CY, Lin CC, *et al*. A recently described type 2 conventional dendritic cell (cDC2) subset mediates inflammation. *Cell Mol Immunol* 2020;**17**:1215–7. https://doi.org/10.1038/s41423-020-0511-y
31. Hartmann E, Graefe H, Hopert A, *et al*. Analysis of plasmacytoid and myeloid dendritic cells in nasal epithelium. *Clin Vaccine Immunol* 2006;**13**:1278–86. https://doi.org/10.1128/CVI.00172-06
32. Sun X, Hosomi K, Shimoyama A, *et al*. International immunopharmacology TLR4 agonist activity of *Alcaligenes* lipid a utilizes MyD88 and TRIF signaling pathways for efficient antigen presentation and T cell differentiation by dendritic cells. *Int Immunopharmacol* 2023;**117**:109852. https://doi.org/10.1016/j.intimp.2023.109852
33. Ushach I, Zlotnik A. Biological role of granulocyte macrophage colony-stimulating factor (GM-CSF) and macrophage colony-stimulating factor (M-CSF) on cells of the myeloid lineage. *J Leukoc Biol* 2016;**100**:481–9. https://doi.org/10.1189/jlb.3RU0316-144R
34. Lutz MB, Strobl H, Schuler G, *et al*. GM-CSF monocyte-derived cells and langerhans cells as part of the dendritic cell family. *Front Immunol* 2017;**8**:1–11.
35. Feng M, Zhou S, Yu Y, *et al*. Regulation of the migration of distinct dendritic cell subsets. *Front Cell Dev Biol* 2021;**9**:1–13.
36. Mata-Haro V, Cekic C, Martin M, *et al*. The vaccine adjuvant monophosphoryl lipid A as a TRIF-biased agonist of TLR4. *Science* 2007;**316**:1628–32. https://doi.org/10.1126/science.1138963
37. Johnson RS, Her GR, Grabarek J, *et al*. Structural characterization of monophosphoryl lipid A homologs obtained from *Salmonella minnesota* Re595 lipopolysaccharide. *J Biol Chem* 1990;**265**:8108–16.
38. Casella CR, Mitchell TC. Inefficient TLR4/MD-2 heterotetramerization by monophosphoryl lipid A. *PLoS One* 2013;**8**:e62622–21. https://doi.org/10.1371/journal.pone.0062622
39. Tanimura N, Saitoh SI, Ohto U, *et al*. The attenuated inflammation of MPL is due to the lack of CD14-dependent tight dimerization of the TLR4/MD2 complex at the plasma membrane. *Int Immunol* 2014;**26**:307–14. https://doi.org/10.1093/intimm/dxt071
40. Stebegg M, Kumar SD, Silva-Cayetano A, *et al*. Regulation of the germinal center response. *Front Immunol* 2018;**9**:1–13.
41. Pai S, Muruganandah V, Kupz A. What lies beneath the airway mucosal barrier? Throwing the spotlight on antigen-presenting cell function in the lower respiratory tract. *Clin Transl Immunol* 2020;**9**:1–13.
42. Vander Lugt B, Khan AA, Hackney JA, *et al*. Transcriptional programming of dendritic cells for enhanced MHC class II antigen presentation. *Nat Immunol* 2014;**15**:161–7. https://doi.org/10.1038/ni.2795
43. Jakubzick C, Helft J, Kaplan TJ, *et al*. Optimization of methods to study pulmonary dendritic cell migration reveals distinct capacities of DC subsets to acquire soluble versus particulate antigen. *J Immunol Methods* 2008;**337**:121–31. https://doi.org/10.1016/j.jim.2008.07.005
44. McAdam AJ, Schweitzer AN, Sharpe AH. The role of B7 co-stimulation in activation and differentiation of CD4+ and CD8+ T cells. *Immunol Rev* 1998;**165**:231–47. https://doi.org/10.1111/j.1600-065x.1998.tb01242.x
45. Iezzi G, Sonderegger I, Ampenberger F, *et al*. CD40-CD40L cross-talk integrates strong antigenic signals and microbial stimuli to induce development of IL-17-producing CD4+ T cells. *Proc Natl Acad Sci USA* 2009;**106**:876–81. https://doi.org/10.1073/pnas.0810769106
46. Milpied PJ, McHeyzer-Williams MG. High-affinity IgA needs TH 17 cell functional plasticity. *Nat Immunol* 2013;**14**:313–5. https://doi.org/10.1038/ni.2567
47. Christensen D, Mortensen R, Rosenkrands I, *et al*. Vaccine-induced Th17 cells are established as resident memory cells in the lung and promote local IgA responses. *Mucosal Immunol* 2017;**10**:260–70. https://doi.org/10.1038/mi.2016.28
48. Guzik TJ, Skiba DS, Touyz RM, *et al*. The role of infiltrating immune cells in dysfunctional adipose tissue. *Cardiovasc Res* 2017;**113**:1009–23. https://doi.org/10.1093/cvr/cvx108

49. Kanneganti TD, Dixit VD. Immunological complications of obesity. *Nat Immunol* 2012;**13**:707–12. https://doi.org/10.1038/ni.2343
50. Juge-Aubry CE, Somm E, Pernin A, *et al*. Adipose tissue is a regulated source of interleukin-10. *Cytokine* 2005;**29**:270–4. https://doi.org/10.1016/j.cyto.2004.10.017
51. Soedono S, Cho KW. Adipose tissue dendritic cells: critical regulators of obesity-induced inflammation and insulin resistance. *Int J Mol Sci* 2021;**22**:8666. https://doi.org/10.3390/ijms22168666
52. Zhuang CL, Lin ZJ, Bi ZF, *et al*. Inflammation-related adverse reactions following vaccination potentially indicate a stronger immune response. *Emerg Microbes Infect* 2021;**10**:365–75. https://doi.org/10.1080/22221751.2021.1891002
53. Cook IF. Subcutaneous vaccine administration—an outmoded practice. *Hum Vaccin Immunother* 2021;**17**:1329–41. https://doi.org/10.1080/21645515.2020.1814094
54. Brown CC, Gudjonson H, Pritykin Y, *et al*. Transcriptional basis of mouse and human dendritic cell heterogeneity. *Cell* 2019;**179**:846–863.e24. https://doi.org/10.1016/j.cell.2019.09.035
55. Tiberio L, Del Prete A, Schioppa T, *et al*. Chemokine and chemotactic signals in dendritic cell migration review-article. *Cell Mol Immunol* 2018;**15**:346–52. https://doi.org/10.1038/s41423-018-0005-3
56. Nakano H, Lyons-Cohen MR, Whitehead GS, *et al*. Distinct functions of CXCR4, CCR2, and CX3CR1 direct dendritic cell precursors from the bone marrow to the lung. *J Leukoc Biol* 2017;**101**:1143–53. https://doi.org/10.1189/jlb.1A0616-285R
57. Gibaldi D, Vilar-Pereira G, Pereira IR, *et al*. CCL3/macrophage inflammatory protein-1α is dually involved in parasite persistence and induction of a TNF- and IFNγ-enriched inflammatory Milieu in *Trypanosoma cruzi*-induced chronic cardiomyopathy. *Front Immunol* 2020;**11**:1–21.
58. Chang TT, Chen JW. Emerging role of chemokine CC motif ligand 4 related mechanisms in diabetes mellitus and cardiovascular disease: friends or foes? *Cardiovasc Diabetol* 2016;**15**:1–8.
59. Perros F, Lambrecht BN, Hammad H. TLR4 signalling in pulmonary stromal cells is critical for inflammation and immunity in the airways. *Respir Res* 2011;**12**:1–8.
60. Marx C, Gardner S, Harman RM, *et al*. Mesenchymal stromal cell-secreted CCL2 promotes antibacterial defense mechanisms through increased antimicrobial peptide expression in keratinocytes. *Stem Cells Transl Med* 2021;**10**:1666–79. https://doi.org/10.1002/sctm.21-0058
61. Jing H, Yen JH, Ganea D. A novel signaling pathway mediates the inhibition of CCL3/4 expression by prostaglandin E2. *J Biol Chem* 2004;**279**:55176–86. https://doi.org/10.1074/jbc.M409816200
62. Randolph GJ, Inaba K, Robbiani DF, *et al*. Differentiation of phagocytic monocytes into lymph node dendritic cells *in vivo* differentiate into DCs in an *in vitro* model of transendo-thelial trafficking without addition of exogenous cyto-kines (Randolph *et al*. 1998), supporting the idea that most ef. *Immunity* 1999;**11**:753–61. https://doi.org/10.1016/s1074-7613(00)80149-1